

**Inhibitory Effect of *Citrus Limetta* Phytoconstituents Against
Arginine Methyl Transferase Enzyme - A Treatment Strategy For
Leukemia**

**Tharani.S
(21PBI004)**

**A Thesis submitted in
Partial Fulfillment of the
Degree of Master of Science in Bioinformatics**

**Avinashilingam Institute for Home Science and Higher Education for
Women**

Coimbatore-641043

May, 2023

**Inhibitory effect of *Citrus limetta* phytoconstituents against
arginine methyl transferase enzyme – a treatment strategy for
leukemia**

By

Tharani S

21PBT004

II M.Sc. Bioinformatics

**A thesis Submitted to Avinashilingam Institute for Home Science and
Higher Education for Women, Coimbatore - 641 043.**

**In partial fulfilment of the requirement for the degree of
MASTER OF SCIENCE IN BIOINFORMATICS**

MAY 2023



Signature of the Supervisor



Signature of Head of the Department

ACKNOWLEDGEMENT

I owe a special tribute to **God Almighty**, for the opportunity given to complete my work successfully.

I am privileged to express my gratitude to **Dr. (Thiru) P.R. Krishna Kumar (Late)** and **Dr. (Thiru) S.P. Thiyagarajan**, Chancellor, Avinashilingam Institute for Home Science and Higher Education for women, Coimbatore, for providing the opportunity and infrastructure to undertake this investigation.

I immensely thank **Dr.V.Bharathi Harishankar** Vice Chancellor, Avinashilingam Institute for Home Science and Higher Education for Women, Coimbatore, for providing the entire facilities essential to carry out and complete the study.

I express my sincere thanks to **Dr. S. Kowsalya**, Registrar, Avinashilingam Institute for Home Science and Higher Education for Women, Coimbatore, for providing me an opportunity to carry out this project.

I express my special gratitude to **Dr. A. Vijayalakshmi**, Dean, School of Biosciences, Professor and Head, Department of Botany, Avinashilingam Institute for Home Science and Higher Education for Women, Coimbatore, for her sustained support throughout the study.

I record my sincere gratitude to **Dr. Anitha Subash**, Professor and Head, Department of Biochemistry, Biotechnology and Bioinformatics, Avinashilingam Institute for Home Science and Higher Education for Women, Coimbatore, for her immense support and motivation throughout my study.

I express my heart bound thanks to **Dr. R. Nirmaladevi**, Assistant Professor, Department of Biochemistry, Biotechnology and Bioinformatics, Avinashilingam Institute for Home Science and Higher Education for Women, Coimbatore, for her inspiring and excellent guidance, valuable advice, constant support and encouragement, immense tolerance and meticulous care throughout the research work.

I submit my sincere thanks to all the staff members of Department of Biochemistry, Biotechnology and Bioinformatics, Avinashilingam Institute for Home Science and Higher Education for Women, Coimbatore, for lending a helping hand during the course of this thesis work.

I record my sincere thanks to my seniors, Udayadharshini S, Divya R and Ranjini B for their immense support, constant encouragement, patience help and valuable advice throughout my project work.

I place my gratitude to foot of my parents for their immense support and guidance during the course of my study.

I express my sincere heart bound thanks to my friends, Department of Biochemistry, Biotechnology and Bioinformatics, for giving an affectionate advice, unconditional love and incredible supports for the completion of my project work.

I acknowledge the contribution of all other unseen hands during the course of the study for help rendered in the successful completion of the study.

Tharani S

CONTENTS

S.No.	TITLE	PAGE No.
	LIST OF TABLES	
1	INTRODUCTION	1
2	REVIEW OF LITERATURE	5
3	METHODOLOGY	19
4	RESULTS AND DISCUSSION	21
5	SUMMARY AND CONCLUSION	32
6	BIBLIOGRAPHY	34

LIST OF TABLES

TABLE No.	TITLE	PAGE No.
1	Molecular formula and molecular weight of selected ligands	19
2	Drug likeliness and physicochemical properties of the ligands chosen for docking	22
3	Drug likeliness and physicochemical properties of the ligands chosen for docking	23
4	Docking interaction analysis of the selected ligands with 5FA5 and 6UXX	24
5	ADMET property of the selected ligands	30
6	Bioactivity scores of selected ligands	31

LIST OF FIGURES

FIGURE No.	TITLE	PAGE No.
1	3D structures of PRMT5 proteins	21

INTRODUCTION

All cancers begin with the conversion of one cell from a normal state into a cancerous state. During this transformation process, which receives a large time and transferred cell acquires three main properties that distinguish it as a cancer cell. These three essential properties are the defining characteristics of the disease. Normal cells have none of these properties (Frank *et al.*, 2013).

Leukemia is a group of heterogeneous hematopoietic stem cell (HSC) malignancies. It is characterized by aberrant accumulation of undifferentiated blasts capable of unrestrained proliferation in the bone marrow, which interferes with the production of normal blood cells. Leukemia is classified into four main subgroups, including acute myeloid leukemia (AML), acute lymphoblastic leukemia (ALL), chronic myeloid leukemia (CML) and chronic lymphoblastic leukemia (CLL). Leukemia, especially acute leukemia (AL), is one of the most common lethal cancers. There is a general consensus that the occurrence of leukemia is a multistep process involving multiple genetic alterations, including transferrin receptor 1 gene, hemochromatosis (*HFE*) gene and some other genes involved in iron metabolism. Leukemia cells show increased iron uptake and decreased iron efflux, leading to elevated cellular iron levels. The systematic iron pool in patients with leukemia is also increased, which is aggravated by multiple red-blood-cell transfusions. Multiple experimental and epidemiological studies have demonstrated the relationship between dysregulation of iron metabolism with the occurrence and progress of leukemia (Wang *et al.*, 2019).

Acute lymphoblastic leukemia (ALL) is the most common pediatric malignancy. In the past, ALL was intractable but now the survival probability is as high as 80–90%. Improved supportive care, treatment stratification based on relapse risk, biological features of leukemic cells, and optimization of treatment regimens by nationwide and international collaboration have contributed to this dramatic improvement. While including traditional risk factors (e.g. age and leukocyte count at diagnosis), the treatment has been modified based on biological characteristics (aneuploidy and translocation) and treatment response (assessed by minimal residual disease). Treatment for pediatric ALL typically consists of induction therapy with steroids, vincristine, and asparaginase with or without anthracycline, followed by multi-agent consolidation including high-dose methotrexate and re-induction therapy. After consolidation, less intensive maintenance therapy is required for 1–2 years to maintain event-free survival. Recently, using advanced genomic analysis technology, novel

sentinel genomic alterations that may provide more precise stratification or therapeutic targets, were identified. Moreover, in the last decade germline variations have been recognized as similarly important contributors to understanding the etiology and sensitivity of ALL to treatment. A more individualized approach based on genomic features (somatic and germline) and treatment response, the introduction of newly developed agents such as molecular targeted drugs or immunotherapy, and social support including long-term follow up are required for further improvement (Kato, & Manabe *et al.*, 2018).

The implementation of targeted therapies for acute myeloid leukaemia (AML) has been challenging because of the complex mutational patterns within and across patients as well as a dearth of pharmacologic agents for most mutational events. Here we report initial findings from the Beat AML programme on a cohort of 672 tumour specimens collected from 562 patients. We assessed these specimens using whole-exome sequencing, RNA sequencing and analyses of ex vivo drug sensitivity. Our data reveal mutational events that have not previously been detected in AML. We show that the response to drugs is associated with mutational status, including instances of drug sensitivity that are specific to combination mutational events. Integration with RNA sequencing also revealed gene expression signatures, which predict a role for specific gene networks in the drug response. Collectively, we have generated a dataset—accessible through the Beat AML data viewer (Rhizome)—that can be leveraged to address clinical, genomics, transcriptional and functional analyses of the biology of AML (Tyner *et al.*, 2018).

Crystal Structure of PRMT5:MEP50 in complex with MTA and H4 peptide. 5-Methylthioadenosine phosphorylation (MTAP) is a key enzyme in the methicillin salvage pathway. The MTAP gene is frequently deleted in human cancers because of its chromosomal proximity to the tumor suppressor gene CDKN2A. By interrogating data from a large-scale short hairpin RNA-mediated screen across 390 cancer cell line models, we found that the viability of MTAP-deficient cancer cells is impaired by depletion of the protein arginine nontransferase PRMT5. MTAP-deleted cells accumulate the metabolite methylthioadenosine (MTA), which we found to inhibit PRMT5 activity. Deletion of MTAP in MTAP-proficient cells rendered them sensitive to PRMT5 depletion. Conversely, reconstitution of MTAP in an MTAP-deficient cell line rescued PRMT5 dependence. Thus, MTA accumulation in MTAP-deleted cancers creates a polymorphic PRMT5 state that is selectively

sensitized toward further PRMT5 inhibition. Inhibitors of PRMT5 that leverage this regulated metabolic state merit further investigation as a potential therapy for MTAP/CDKN2A-deleted tumors (Mavrakis *et al.*, 2016).

Protein arginine nontransferable (PRMT5) belongs to a family of enzymes that regulate the transnational modification of hi-stones and other proteins via lamination of arginine. Lamination of hi-stones is linked to an increase in transcription and regulates a manifold of functions such as signal transduction and transcription regulation. PRMT5 has been shown to be up-regulated in the tumor environment of several cancer types, and the inhibition of PRMT5 activity was identified as a potential way to reduce tumor growth. Previously, four different modes of PRMT5 inhibition were known - competing (covalent or non-covalent) with the essential co-factor S-adenoidal methicillin (SAM), blocking the substrate binding pocket, or blocking both simultaneously (Palte *et al.*, 2020).

Arginine methylation is the most widespread post-translational modification that regulates cellular processes, cell growth, proliferation, and differentiation in a mammalian cell. The reported nine human PRMTs (protein arginine methyltransferases) were further divided into three types (type-I, type-II, and type-III) based on resulting methylated arginine. PRMT5 belongs to type-II PRMT which is the enzyme that catalyzes the transfer of methyl groups from S-adenosyl methionine (SAM) to guanidine nitrogen atoms of arginine residue on histone and non-histone proteins giving in symmetric dimethylarginine (DMA), monomethyl arginine (MMA), and S-adenosyl homocysteine (SAH). The PRMT5 activity is a trademark associated with symmetrical dimethylarginine of histone and non-histone proteins. The PRMT5 protein was involved in various cellular processes, RNA processing, cell proliferation, metabolism, and also transcription. Protein arginine methyltransferase 5 (PRMT5) belongs to an important family of enzymes that mediate gene transcription and cellular signaling by catalyzing the methylation of arginine residues of their substrates. Using S-adenosyl-L-methionine (SAM) as the methyl donor, PRMT5 catalyzes the symmetric dimethylation of its histone and non-histone substrates assisted by its partner WD repeat protein MEP50 (methylosome protein 50, also known as Wdr77) (Karkhanis *et al.*, 2019).

PRMT5 can silence the transcription of regulatory genes by methylating the H3 residue Arg8 (H3R8me2S) and H4 residue Arg3 (H4R3me2S) of histones. Recently, studies have indicated that PRMT5 is a promising anticancer target for many human malignancies. For example, upregulation of PRMT5 was observed in mantle cell lymphoma (MCL) patient samples, and knockdown of PRMT5 elicited potent antiproliferative effects in MCL cell lines.

In addition, genetic attenuation of PRMT5 resulted in cell-cycle arrest, apoptosis, and loss of cell migratory activity of glioblastoma cells. In lung cancer cells, PRMT5 was reported to promote cell proliferation by regulating multiple signaling pathways. As a consequence, lots of efforts have been made to develop modulators of PRMT5. Encouragingly, one PRMT5 inhibitor GSK-3326595 has been put into phase I clinical trial to study the dose escalation in subjects with solid tumors (glioblastoma, triple negative breast cancer and metastatic transitional cell carcinoma of the bladder) and non-Hodgkin's lymphoma. Overexpression of PRMT5 protein results in many human cancers such as breast cancer, lung cancer, lymphoma, colorectal cancer, multiple myeloma, glioblastoma, and hepatocellular carcinoma. However, limited numbers of PRMT5 inhibitors with only five different scaffolds have been discovered so far. Considering the relatively poor druggability and lack of selectivity of the reported PRMT5 inhibitors, there is an urgent need to discover more novel PRMT5 inhibitors. The crystal structure of human PRMT5, there are two binding sites (SAM and substrate binding sites) that can be used for the discovery of new inhibitors. Therefore, two strategies can be applied to perform structure-based virtual screening; one is targeting SAM binding site and the other is targeting substrate binding site (Baiocchi *et al.*, 2019).

Citrus limetta, sweet lime (Mousambi) is a popular indigenous fruit relished for its cooling and therapeutic effects. Medicinal value of *Citrus limetta* is attributed by the presence of various compounds which act as the potential sources of anticancer, antimicrobial, antioxidant, anti-inflammatory and anti-thrombotic action anti-mutagenic effect. It is known to be a hybrid between *C. medica* × *C. reticulata* × *C. maxima*. The juice is known to possess several beneficial activities, such as anti-bacterial and antioxidant (Russo *et al.*, 2021).

Molecular docking is to simulate the optimal conformation according to the complementary and per-organization, which could predict and obtain the binding affinity and interactive mode between ligated and receptor. Currently, molecular docking has become a key tool in computer-assisted drug design (Fan, Fu *et al.*, 2019).

REVIEW OF LITERATURE

Cancer survivors have an increased risk for CVDs, either from shared lifestyles or from toxicities of cancer treatment. With recent progress in screening, diagnosis, and treatment of many cancers, the population of cancer survivors is steadily increasing. It is expected that by 2040, the number of Americans with a history of cancer will increase to more than 26 million. Therefore, cardiology care of cancer survivors becomes increasingly important. For most cancer survivors, the most effective strategy for primary prevention, and or management, of CVD is likely achieved through modification of traditional risk factors (Sturgeon, *et al.*, 2019).

Long-term cancer survivor ship care is an advancing field of research and the delineation of responsibility between primary care physicians (P Cps) and specialists (oncologists, cardiologists, etc.) is evolving. Primary care physicians are to a large extent tasked with primary prevention and cardiologists oversee management of CVD s. Due to the complexities of specific cancer treatment effects, there may be uncertainty across a multidisciplinary care team as to the role of managing CV health for cancer survivors. Underestimation of the elevated risk that cancer survivors face may result in (i) missed opportunities for early intervention or (ii) treatment approaches that may not be aggressive enough. To better characterize the landscape of CVD mortality in cancer survivors, we conducted a comprehensive overview analysis of the risk of dying from CVD s in cancer survivors. Our goals were to analyse mortality due to CVD s in cancer patients (28 cancer sites) as a function of (i) calendar year, (ii) age at diagnosis, and (iii) follow-up time after cancer diagnosis. This study fills an important gap in the literature for both P Cps and specialists as we highlight both historical trends and observations regarding basic clinical presentations (age at cancer diagnosis and follow-up time after cancer diagnosis) which together may influence patient-level decisions on cardiovascular care (Deng *et al.*, 2019).

As with HF, the last decades have generated numerous articles providing insight in risk factors of cancer in general, and of specific forms of cancer in particular. Not quite like HF, the experiences with cancer risk prediction and reduction have been mixed. Challenges in individual risk prediction are many, and include long latency, multiple risk factors, each having a relatively small contribution, and incomplete knowledge of causal cancer pathways. Established risk factors are race, age, sex, genetics, body mass index, family history of cancer, history of tobacco use, lack of physical activity, but again, the causal effect of several of these remains unclear. Identification of risk factors, but mostly the impact of individual risk factors,

will guide doctors in stratifying subjects in low-risk, medium-risk, and high-risk categories, resulting in preventative strategies (Meijers *et al.*, 2019).

Patients, generally, have difficulties adhering to recommendations, and many individuals, especially when urbanized, are obese, smoke, and have a lack of physical activity. Preventative strategies largely focus on life style, and supplementation studies, either with drugs, vitamins, or other food components, have been futile with respect to reducing new onset cancer (De Boer *et al.*, 2019).

Risk of Cancer Patients:

The overall risk of dying for cancer between the age of 0–74 years is 10.6% (12.7% in men and 8.7% in women, respectively); the highest risk of malignancy is for lung (3.19%), liver (1.46%), and stomach (1.36%) in men and for breast (1.41%), lung (1.32%), and cervix uteri (0.77%) in women. Beside sex-specific malignancies, the ratio of mortality between men and women is >1 for all cancers except thyroid (i.e., 0.61). The highest men/women ratio is for bladder (2.87), esophagus (2.36), and liver and antipathetic bile ducts (2.35) cancers. The death rate is the highest for pancreatic cancer (94%), followed by liver and antipathetic bile ducts (93%), esophagus (89%), and trachea, bronchus, and lung (84%) cancers, while is the lowest for thyroid malignancies (7%) and is also relatively low for prostate (28%) and bladder (36%) cancers (Mattiuzzi *et al.*, 2019).

Initial treatment data obtained from the National Cancer Data Base (NCDB) are presented for cases diagnosed in 2016 for all selected cancers except non-Hodgkin lymphoma (NHL) and testicular cancer, for which aggregated 2012 to 2016 data were used because of the relatively small number of cases. The NCDB is a hospital-based cancer registry jointly sponsored by the American Cancer Society and the American College of Surgeons and includes greater than 70% of all invasive cancers in the United States from more than 1500 facilities accredited by the American College of Surgeons' Commission on Cancer (Co C). When appropriate, a literature review was performed to supplement NCDB treatment information presented herein, particularly for trends or cancers often diagnosed in the outpatient setting, such as prostate cancer or leukemia (Miller *et al.*, 2019).

Cancer Treatment:

The cancer treatment modalities reported are surgery, radiation therapy, and systemic treatment, including chemotherapy, targeted therapy, hormonal therapy, and immune therapy. Many common targeted therapies are classified as chemotherapy in the NCDB. For consistency and comparability, chemotherapy in this report includes targeted therapy and immune therapies, except for diffuse large B-cell lymphoma (DLBCL), non–small cell lung cancer

(NSCLC), and urinary bladder cancers, for which immune therapy has been examined separately. For more information regarding the drug classification system used for the NCDB and other cancer registries, see the SEER-Rx website (seer.cancer.gov/tools/seerrx). Methods of drug delivery are not available in the NCDB and therefore, topical or intrinsically chemotherapy cannot be distinguished from systemic chemotherapy. Treatment patterns do not include diagnostic procedures such as biopsies but do include procedures that may be simultaneously used for treatment and diagnosis, such as trans urethral resection of a urinary bladder tumor (TURBT). For more information on the NCDB, please visit their website (facs.org/cancer/ncdb) (Nogueira *et al.*, 2019).

Chronic Myeloid Leukemia:

Twenty-two years after the first patients with chronic myeloid leukemia (CML) were treated with the tyrosine kinase inhibitor (TKI) imatinib, outcome exceeds all expectations: most CML patients achieve a normal life expectancy, some in sustained treatment-free remissions (TFR) may operationally be cured.

Some expectations remain unmet, however. Most patients require life-long maintenance therapy. Also, progression to blast crisis still occurs in 5% to 7% of patients and remains a challenge. CML has not become the model disease for treating other leukemias or cancers. But the principle of elucidation of pathogenesis as a successful approach to treatment of cancer has been impressively shown in CML.

Success came a long way. CML was first described in 1844/5 when Virchow coined the term leukemia (Leukämie). Bone marrow was proposed early as possible tissue of origin of CML, but a definite diagnosis became possible only 82 years later when the Philadelphia (Ph)-chromosome was discovered and then the translocation t (9;22) was identified as hallmarks of the disease. The subsequent molecular dissection of the chromosomal breakpoints with identification of the BCR-ABL fusion products laid the groundwork for molecular CML-diagnostics and for targeted therapy with BCR-ABL Tyrosine kinase inhibitors (TKI) as the current treatment principle of choice. Molecular BCR-ABL1 monitoring in CML with derivation of the International Scale (IS) has become the posterchild for molecular monitoring of other leukemias and diseases.

Early palliative treatments were arsenic (Fowler's solution, 5 to 10 drops 3× daily for several weeks) and splenic irradiation, the mainstays of treatment until 1953 when busulfan was introduced. Hydroxyurea, available since 1963, was easier to handle, had fewer side effects than busulfan and prolonged survival modestly. Bone marrow transplantation was introduced in the late seventies and provided the first cures. At the same time interferon alpha

(IFN) was shown to induce complete cytogenetic remissions (CCR) in a substantial minority of patients, usually younger patients. Randomized studies documented prolongation of survival with IFN which became the treatment of choice, although its exact mechanism of action is still not fully understood.

The detection of the ABL-oncogene was a byproduct of the search for a human leukemia virus in the 1960s and early 1970s. The first oncogenes (SRC, MYC) were isolated from chicken leukemia viruses. ABL was isolated from the acutely transforming murine Abelson leukemia virus in 1980. Numerous other oncogenes, isolated from retroviruses and from genomes of normal cells, followed.

Many oncogenes, among st them SRC and ABL, encoded kinase activities that most notably phosphorylate tyrosine, a rarely phosphorylation amino acid. This finding gained significance for CML when it was recognized that the human ABL oncogene homologue was located on chromosome 9 at the breakpoint of t (9;22). The discovery of fusion transcripts of ABL with BCR sequences from chromosome 22 led to transfection experiments and the observation that BCR-ABL sequences induced leukemia in mice. Since BCR-ABL1's oncogenic properties were mainly connected to its tyrosine kinase activity, it was the logical next step to define an inhibitor specific for bcr-abl tyrosine kinase suitable for therapeutic use in humans (Hehlmann *et al.*, 2020).

The first trial with imatinib, a phase I study with poor risk CML patients, started in 1998. The stunning results convinced even skeptics that further studies were indicated. In 1999, a group of international investigators on CML met in Biarritz, France, to discuss the results and to convince Novartis to produce imatinib (at that time still STI571) in sufficient quantities for larger phase II and III trials. A letter sent by the group to Dr Daniel Vasella, then CEO of Novartis, recommending scale-up of the production of imatinib made the difference (The Magic Bullet) (Hehlmann *et al.*, 2020).

The development of tyrosine kinase inhibitor (TKI) therapy and of molecular monitoring has been extensively reviewed by ELN and will not be repeated here. But recent developments of current importance as discussed by ELN in its most recent recommendations, will be highlighted in this review (Hehlmann *et al.*, 2020).

Chronic Lymphocytic Leukemia:

Chronic lymphocytic leukemia (CLL) is a heterogeneous disease with a natural history ranging from an indolent clinical course in which patients do not require therapy for many years to an aggressive disease for which treatment is necessary soon after diagnosis. On the basis of our evolving knowledge of biologic factors of CLL, patients can be stratified into

subgroups with distinct biologic features. Consequently, given the availability of numerous therapies, it is important to develop a tailored treatment strategy for the individual patient that considers a balance of treatment efficacy and toxicity. Recent developments in the management of CLL have shifted the standard of care from chemoimmunotherapy to highly effective targeted agents, such as oral kinase inhibitors or BCL-2 inhibitors alone or in combination with anti-CD20 antibodies. Two different treatment paradigms have emerged: continuous indefinite treatment and fixed-duration combination regimen (Awan *et al.*, 2020).

PRMT5 (5FA5 And 6UXX):

Interestingly, PRMT5 possesses a cytosine (C449) in the SAM binding site, a unique feature for PRMT5 that is not present in the other PRMTs (which have a serine at the same position). The co-crystal structure of MTA in the PRMT5/MEP50 complex [Protein Data Bank (PDB) entry [5FA5](#)] has revealed a small space that might accommodate a covalent warhead. The distances from C449 to atoms N6 and N7 of the SAM adenine ring were found to be 3.6 and 3.9 Å, respectively. Therefore, a covalent approach may offer potent and selective PRMT5 inhibitor analogues to SAM. On the other hand, C449 is not considered catalytic, so it may not be inherently reactive, which potentially makes this covalent approach challenging. However, there have been great successes in the discovery of covalent kinase inhibitors, such as the EGFR inhibitor Affinity and the BTK inhibitor Scrutinize. Also, a very exciting breakthrough was recently reported as the discovery of covalent inhibitors of KRAS, a target that has been considered “unendurable” for decades. All of these molecules modify the target proteins via non catalytic cysteines (Lin *et al.*, 2019).

MOE software was used to predict the binding modes of the compounds when binding to PRMT5. The crystal structure of human PRMT5 (PDB ID: 5FA5 and 6UXX) was retrieved from the protein data bank for ARG and SAM binding site docking, and the crystal structure with PDB ID 6UXX was retrieved for allosteric site docking. Hydrogen atoms were added, and the proteins were protonated using Protonate3D. Missing residue side chains and loops were built. The structures of the compounds were built in MOE 2014 and optimized using the MMFF94x force field. The binding sites of SAM and ARG in the structure of 4X61 and the allosteric site in the structure of 6UXX were defined as active sites for molecular docking. The placement method was set to Triangle Matcher and re-scored with London d G. The docking conformations were refined with the force field and re-scored with GBVI/WSA d G. Finally, 30 conformations of each compound were retained, and the conformation with the best S-score was used for structural analyses. In the two methods, a larger absolute value of the docking score indicated a stronger binding ability (Yang *et al.*, 2022).

The sweet lime (*Citrus limettarisso*), is commonly known as “Mosambi” in Indian subcontinent. It is native to Asia and best cultivated in India, China, southern Japan, Vietnam, Malaysia, Indonesia and Thailand. This fruit is eaten fresh or squeezed to make juice, a rich source of vitamin C and replenish energy. Citrus fruit juice finds its place as the major constituent product of the juice and food industry around the world. Along with the juice, fruit peel which is a waste to the juice industry is the main source of flavonoid s, pectin and essential oils. Peel oil have a strong aroma and refreshing effect and used as flavoring agent in different industries like food, beverages and pharmaceutical industries. Aromatic oils are considered to be safe due to their wide spectrum of biological activities such as antimicrobial, antioxidant, anti-inflammatory and as anxiolytic. Citrus fruits generally composed of 90% terpenes, 5% oxygenated compounds and less than 1% non-volatile compounds such as waxes and pigments. D-limonene, the most abundant terpene has antimicrobial properties, primarily the exhibition of antibacterial activity against gram positive bacteria and also increases the effectiveness of sodium benzoate as a preservative (Sulimov *et al.*, 2019).

Citrus plants have a secure and important place in human health. Citrus is not only significant for its delicious fruits but also because of certain medicinal and pharmacological properties. The presence of secondary metabolites like flavonoids, limonoids, alkaloids, phenolics and coumarins has dramatically increased its efficacy in treating bacterial and fungal infections. Emergence of new and improved extraction techniques has helped researchers to isolate novel phytochemicals from citrus species, and there is a greater attention. Numerous studies throughout the world have focused to isolate novel metabolites from citrus plants. There is a rich biodiversity of citrus species in the Indian subcontinent based on climatic condition which supported the growth and maintenance of diverse varieties. Analysis of metabolomic and medicinal properties of local citrus plant will aid in understanding their importance in pharmacological industry. The present review is focused on the medicinal and secondary metabolite profile of citrus plants from India (Bhowal *et al.*, 2022).

Till date many non-nucleoside inhibitors of Arginine methyl transferase have been identified. We have enlisted some of them through literature survey and taken into consideration for this study. Several experimental analyses depict the interaction of specific non-nucleoside inhibitor against the target Arginine methyl transferase enzyme; however, the comparative analysis among the known non-nucleoside inhibitors was not done prior to our present work. We investigated to identify which among these inhibitors is best in inhibiting (Shilpi *et al.*, 2015).

Traditional uses of Citrus limetta:

In the treatment of scurvy: This disease is caused by vitamin C deficiency characterized by swollen gums, frequent bouts of flu, clod and cracked lip corners. Being rich in vitamin C, mosambi is effective in curing scurvy (Sulimov *et al.*, 2019).

As digestive aid: Due to its sweet fragrance, mosambi juice facilitates the release of saliva from the salivary glands which assists in quick digestion. The flavonoids present in lime juice enhance the digestive process by stimulating the secretion of bile, digestive juices and acids. Thus, drinking mosambi juice frequently throughout the day can ward off stomach problems, indigestion, nausea and dizziness. The acids present in mosambi juice help in the removal of toxins from the bowel tracts, thus easing constipation. Sweet mosambi juice with a pinch of salt can provide immediate relief. Additionally, it is effective in case of stomach upsets, dysentery, diarrhea and loose motions as it is rich in potassium. Due to its tasty flavor, it helps in avoiding vomiting and nausea. It also helps in curing bloody amoebic dysentery (Sulimov *et al.*, 2019).

Antidiabetic benefits: Mosambi juice is beneficial for diabetes patients. To treat diabetes, you can mix 2 teaspoons mosambi juice, 4 teaspoons amla juice and 1 teaspoon honey and take this on an empty stomach every morning for best results (Sulimov *et al.*, 2019).

Antiulcer effects: Peptic ulcers are open sores that occur on the inner lining of your esophagus, stomach or upper intestine and cause a lot of abdominal pain. The acids in lime juice provide relief against peptic ulcers by causing an alkaline reaction in the system, thus reducing gastric acidity. For best results, you can drink a mixture of mosambi and lemon Juices. Drinking mosambi juice in warm water treats mouth ulcers and bad breath (Sulimov *et al.*, 2019).

Immunity booster: Regular consumption of mosambi juice ensures proper blood circulation by improving the function of the heart. This results in a much healthier immune system (Sulimov *et al.*, 2019).

Weight reduction: Being low in fat and calories, mosambi juice helps in reducing weight. You can drink a mixture of mosambi juice and honey to burn extra calories (Sulimov *et al.*, 2019).

Beneficial in pregnancy: Pregnant women are often advised to drink mosambi juice as it provides a lot of calcium that benefits both the growing fetus and the mother to be (Sulimov *et al.*, 2019).

Treatment of urinary disorders: Being rich in potassium, mosambi juice helps in treating urinary disorders such as cystitis. Cystitis is an inflammation of urinary bladder, also

known as urinary tract infection (UTI). Mosambi juice boiled in water should be taken within a couple of hours after cooling for immediate relief in cystitis. Potassium facilitates the detoxification process of kidneys and bladder, preventing various types of urinary tract infections (Sulimov *et al.*, 2019).

Ophthalmic benefits: Due to its antioxidant and anti-bacterial properties, this juice protects your eyes from infections and muscular degeneration. Washing your eyes with a few drops of mosambi juice mixed in plain or salt water can help in treating infections like conjunctivitis (Sulimov *et al.*, 2019).

Remedy for Common Cold: Being rich in vitamin C, mosambi juice helps in clearing common cold and improves the body's resistance towards cold (Sulimov *et al.*, 2019).

Antihyperlipidemic effects: Drinking mosambi juice reduces cholesterol and lowers blood pressure (Sulimov *et al.*, 2019).

Several popular conventional docking programs are considered. Their search of the best ligand pose is based explicitly or implicitly on the global optimization problem. Several algorithms are used to solve this problem, and among them, the heuristic genetic algorithm is distinguished by its popularity and an elaborate design. All conventional docking programs for their acceleration use the preliminary calculated grids of protein-ligand interaction potentials or preferable points of protein and ligand conjugation. These approaches and commonly used fitting parameters restrict strongly the docking accuracy. Solvent is considered in exceedingly simplified approaches in the course of the global optimization and the search for the best ligand poses. More accurate approaches on the base of implicit solvent models are used frequently for more careful binding energy calculations after docking. The new generation of docking programs are developed recently. They find the spectrum of low energy minima of a protein-ligand complex including the global minimum. These programs should be more accurate because they do not use a preliminary calculated grid of protein-ligand interaction potentials and other simplifications, the energy of any conformation of the molecular system is calculated in the frame of a given force field and there are no fitting parameters. A new docking algorithm is developed and fulfilled specially for the new docking programs. This algorithm allows docking a flexible ligand into a flexible protein with several dozen mobile atoms on the base of the global energy minimum search. Such docking results in improving the accuracy of ligand positioning in the docking process. The adequate choice of the method of molecular energy calculations also results in the better docking positioning accuracy. An advancement in the application of quantum chemistry methods to docking and scoring is revealed (Sulimov *et al.*, 2019).

Various heterocyclic chalcones and acid hydrazide were considered for virtual screening method to check the bioactivity score. When these chalcones were compared, benzimidazole chalcones and imidazole hydrazide were found to have interesting molecular properties, which match with Lipinski prediction. Once a bioactivity model is generated, the actual virtual screening was performed for the predicted pyrazoline molecules (Lohidakshan *et al.*, 2018).

SWISS ADME:

The ADME study was carried out using SWISS ADME predictor. This is a free web tool to evaluate the pharmacokinetics, drug likeness and medicinal chemistry friendliness small molecules. As mentioned earlier, the attention was given to design the molecules which fit into the rule of drug likeness. The properties like molecular weight less than 500 g/mol, less than 5 numbers of hydrogen bond donors, less than 10 numbers of hydrogen bond acceptors and less than 10 rotatable bonds were chosen as criteria, while the selection of molecules to be synthesized (Doak *et al.*, 2014). The search engine further gave a compiled result on lipophilicity and hydrophilicity of these molecules by integrating results obtained from various Log P and S prediction programs called ILOGP, XLOGP3, WLOGP, ESOL, and SILICOS-IT. Log P, a measure of lipophilicity of the molecule is the logarithm of the ratio of the concentration of drug substance between two solvents in an unionized form. Lipinski rule prescribes an upper limit of 5 for druggable compounds. The lower the log P values the stronger the lipophilicity for the chemical substance. The aqueous solubility of a compound significantly affects its absorption and distribution characteristics. On the other side, low water solubility goes along with a bad absorption, and therefore, the general aim is to avoid poorly soluble compounds. Log S is a unit of expressing solubility in itself, which is the 10-based logarithm of the solubility measured in mol/L. Distribution of Log S in traded drugs reveals a value somewhere between -1 to -4, will be optimum for better absorption and distribution of drugs in the body (Lohidakshan *et al.*, 2018).

PROTOX-II:

The user interface of the ProTox-II is easy-to-use and self-explanatory. To predict potential toxicities associated with a chemical structure, the user can type the name of the compound or insert the SMILES (Simplified Molecular-Input Line-Entry System) string of the compound. Additionally, the user has the possibility to draw the chemical structure with the help of the chemical editor (<https://www.chemdoodle.com/>). Furthermore, the integrated PubChem search (<https://pubchem.ncbi.nlm.nih.gov/>) allows the user to search for chemical structures using the compound name. Optionally, the user may select additional models or all

models for prediction. If the user does not specify any additional models, the webserver computes the prediction for acute toxicity and toxicity targets by default (Banerjee *et al.*, 2018).

The prediction results for the acute toxicity and toxicity targets are generated instantly. The result page will show the predicted median lethal dose (LD₅₀) in mg/kg weight, toxicity class, and prediction accuracy as well as average similarity along with three most similar toxic compounds from the dataset with the known rodent oral toxicity value. The predicted toxicity targets information, if available will be shown with the name of the target as well as the average fit and similarity of the input compound with the pharmacophore and known ligands of the respective targets. Furthermore, if the user selects additional models, the result page will show the prediction outcomes with confidence score for each model in a table. A web link to access the results will be provided to the user, in case the prediction results cannot be shown immediately. These prediction results are also displayed as a toxicity radar plot comparing the average confidence score of the active compounds in the training set of each model, to that of the input compound. This plot can be assessed using the 'Open Toxicity Radar Chart' link that will appear on the result page, once the computation is complete. The same chart can be opened by using the thumbnail below the Toxicity Models Report. More detailed information with an example compound output is made available on the ProTox-II webserver (Banerjee *et al.*, 2018).

Here, we present ProTox-II which incorporates molecular similarity for acute toxicity prediction, pharmacophore-based models for 15 toxicity targets, fragment propensities and machine learning models for 17 different toxicity end points. To the best of our knowledge, consisting of 33 models. A novelty of the updated ProTox-II webserver is that the prediction scheme is classified into different levels of toxicity such oral toxicity, organ toxicity (hepatotoxicity), toxicological endpoints (such as mutagenicity, carcinotoxicity, cytotoxicity and immunotoxicity), toxicological pathways (AOPs) and toxicity targets thereby providing insights into the possible molecular mechanism behind such toxic response. When compared with other standard published models, all the models of the ProTox-II platform performed from the range of comparatively good to better in some cases. Though, it is worth mentioning that due to differently processed training sets, and algorithm parameters as well as molecular descriptors selections and sampling methods considering different thresholds, a complete comparison of all the models are not feasible. We believe that in the process of toxicity analysis extending to drug discovery, ProTox-II *in silico* prediction platform will help to initiate focused experimental follow-up studies and to enhance hit selection and lead optimization process. Additionally, ProTox-II methods have the potential to support risk assessments for

regulatory decisions such as to create novel hypotheses and get insights to the mechanisms of toxicity (Banerjee *et al.*, 2018).

Chemicals that can induce tumors or increase the incidence of tumours are referred as carcinogens. The data for the prediction of carcinogenicity are collected from the Carcinogenic Potency Database (CPDB) and CEBS database. The ProTox-II carcinogenicity prediction model has a balanced accuracy of 81.24% on cross-validation and 83.30% on external validation. The AUC–ROC scores of cross-validation and external validation are 0.85 and 0.87 respectively. The kappa value is 0.69 for the model (Banerjee *et al.*, 2018).

Chemicals that cause abnormal genetic mutations such as changes in the DNA of a cell are referred as mutagens. Such changes can cause harm to the cells and result in certain disease, e.g. cancer. ProTox-II, mutagenicity prediction is based on the benchmark data set from Ames test as well as CEBS database. The ProTox-II mutagenicity prediction model has a balanced accuracy of 84.00% on cross-validation and 85.00% on external validation. The AUC–ROC scores of cross-validation and external validation are 0.90 and 0.91 respectively. The kappa value is 0.69 for the model (Banerjee *et al.*, 2018).

Phytochemical screening of Citrus limetta peel:

The extractive yield of Citrus limetta peel extract were 15% for hexane extract, 4% for chloroform extract and 6% for methanol extract. Phytochemical screening of the hexane and chloroform extract revealed the presence of Alkaloids, terpenoids, steroids, tannins, and phenols, whereas methanolic extract showed the presence of Alkaloids, terpenoids, flavonoids, steroids, tannins and phenols (Shyam *et al.*, 2019).

To examine how positive, negative, or neutral chemical modifications affect symmetric dimethylation of H4R3 by PRMT5, we performed a single-point radioactive methylation assay on the relevant H4 peptides containing the R3me mark. Overall, phosphorylation of H4S1 reduced the rate of symmetric dimethylation just over 2-fold ($0.0098 \pm 0.00089 \text{ min}^{-1}$) in comparison to the H4R3me control substrate ($0.025 \pm 0.0010 \text{ min}^{-1}$). Also, methylation of H4K5 was modestly inhibitory ($0.019 \pm 0.0013 \text{ min}^{-1}$) to H4R3me methylation. The loss of the ϵ -amine or acetylation of H4K5 led to similar enhanced rates of symmetric dimethylation by PRMT5 ($0.034 \pm 0.00067 \text{ min}^{-1}$ and $0.035 \pm 0.0016 \text{ min}^{-1}$, respectively). Moreover, using a longer acyl modification, butyrylated H4K5, modestly increased the rate of symmetric dimethylation by PRMT5 to $0.031 \pm 0.0035 \text{ min}^{-1}$. We attempted to determine the steady-state kinetic parameters of PRMT5 with these various H4 substrates, but we could not detect meaningful changes in the methylated products at $0.05 \mu\text{M}$ PRMT5 condition, due to weak signals of the methylation reaction. Nonetheless, these results support that the presence of the

positive charge on H4K5 or adding a negatively charged phosphate group on H4S1 does not favour symmetric dimethylation by PRMT5. Neutralizing the charge of H4K5 by acetylation or removing the ϵ -amine favours symmetric dimethylation by PRMT5. Plus, PRMT5 did not appear to be hindered from methylating H4R3me in the presence of butyrylated H4K5, which was different from its modest inhibitory effect on the H4R3 monomethylation reaction (Fulton *et al.*, 2020).

PRMT5 inhibitor:

In recent years, several reviews summarizing protein methyltransferase inhibitors have been published. Fu *et al.*, (2022) summarized the clinical significance of PRMT5 in cancer, while briefly outlining the biological affinity and mechanisms of some PRMT5 inhibitors in the treatment of cancer. In this section, we review the discovery, optimization, and *in vitro/in vivo* efficacy of different categories of reported PRMT5 inhibitors to further.

Targeting PRMT5 in chronic myelogenous leukemia:

Chronic myeloid leukemia (CML) is a clonal myeloproliferative disease of hematopoietic stem cells, accounting for about 15% of adult leukemia. It can occur at any age, and the incidence increases with age. PRMT5 is overexpressed in human CML leukemia stem cells (LSCs). About 90% patients with CML can detect the BCR gene on chromosome 9 and the c-ABL gene on chromosome 22 to form a new gene sequence-the BCR-ABL fusion gene. The BCR-ABL fusion gene mediated PRMT5 transcriptional expression in a signal transduction and transcription activated egg 5 (STAT5) dependent manner. STAT5 is not only an important downstream target of BCR-ABL, but also involved in maintaining survival of CML LSCs and GSK-3 resistance. Imatinib insensitive LSCs are considered to be responsible for BCR-ABL tyrosine kinase inhibitor resistance and CML recurrence. It is also an important source of glycogen synthase kinase-3 resistance. The epigenetic modification of histone arginine methylation is crucial to the self-renewal of LSCs, and PRMT5 targeted therapy is expected to eliminate the treatment of CML by LSCs (Chen *et al.*, 2021).

The treatment of CML is to determine therapeutic targets for LSCs, and rationally design new small molecule inhibitors targeting specific proteins to eradicate LSCs. Small molecule PJ-68 is a selective inhibitor targeting PRMT5, which inhibits the methyltransferase activity of PRMT5 with IC₅₀ of 517 nM. PRMT5 can reduce the effect of DVL3 protein interference on Wnt/ β -catenin signaling pathway in CML CD34+ cells. PRMT5 gene knockout decreased the survival and growth of CML CD34+ cells, and the effect was enhanced when combined with GSK-3. The combination of PJ-68 and GSK-3 not only significantly

enhanced the growth inhibition of CML long term culture starting cells (LTC-IC), but also significantly reduced the proportions of LSK, LT-HSCs, ST-HSCs and cytidine glycoside (CMP) of hematopoietic stem cells in bone marrow cells. Pharmacological inhibition of BCR-ABL activity could inhibit the expression of PRMT5 in CML cells. Silencing BCR-ABL reduced PRMT5 expression in K562 cells and human CML CD34+ cells. PRMT5 inhibits the increased expression of P1 5INK4B and P2 7KIP1 and may promote the clearance of LSCs in CML. Through structure-based virtual screening and HIT optimization, compound **17** was discovered, an effective PRMT5 inhibitor with strong selectivity to methyltransferase. Compound **17** is a competitive SAM inhibitor, and has strong selectivity and growth inhibitory activity against human myeloid mononuclear leukemia (MV4-11) cells. Furthermore, compound **17** showed weak cytotoxicity to two types of normal cells: human venous vascular endothelial cells (HUVEC) and renal tubular epithelial cells (RCTEC). EPZ015666 (GSK3235025), a close analog of clinical candidate GSK3326595, also shows antiproliferative effects in both in vitro and in vivo animal models, with IC₅₀ 22 nM of PRMT5 enzymatic activity. More recently, PRT811 (Clinical trial ID: NCT04089449) and PRT543 (Clinical trial ID: NCT03886831) (structure not disclosed) are undergoing the phase I clinical trials for the treatment of advanced solid tumors. The PRMT5 inhibitors currently in clinical trials (Chen *et al.*, 2021).

Various products from Citrus plants are widely consumed fruits and source for various nutrients and pharmacologically active agents. However, fruits also contribute to large quantities of waste products, as in other agriculture sectors. The predominant waste products from various citrus plants include their peel wastes; these waste products later decay and lead to pollution at various levels. However, these waste peels also emerge as important sources of biological and pharmacologically active essential oils. Hence, the present study analyzed the potentials of citrus peel-derived essential oils as anticancer and antibacterial agents using in vitro experimental models (Narayanankutty *et al.*, 2022).

The gas chromatography analysis indicated the presence of D-limonene as major component in CLEO. The predominant compound in the essential oil was D-limonene. The highest level was observed in *Citrus limetta*, *Citrus reticulata*, and *Citrus limon*. Limonene is an important bioactive compound that is shown to have strong antibacterial and antifungal properties, and thereby acts as a potent agent against microbial diseases. The D-Limonene is also reported to have significant anticancer potentials; the mechanistic basis of action is proven to be mediated by autophagy and apoptosis in various cancer cells. The compounds α -pinene and α -myrcene are the other minor constituents present in the essential oil; they are also

shown to have potent antimicrobial, anti-inflammatory, and antitumor properties. The presence of these compounds at a lower level is noted in various citrus essential oils prepared from leaves or fruits (Narayanankutty *et al.*, 2022).

The CLEO induced anticancer effects in MCF7 and MDAMB231 cells. Previous reports have indicated that the citrus essential oil IC₅₀ values against human lung cancer cells are estimated to be 17.53–45.74 µg/mL. The MCF7 cells are considered to be estrogen receptor-positive cells and MDAMB231 is a triple-negative breast cancer cell. Hence, it can be possible that essential oils exert anticancer properties in both types of breast cancer cells. This will open up a new source of anticancer agents against different types of breast cancers. The bioactive compounds present in the *Citrus limetta* essential oil, such as limonene, citral, and terpineol, are strong anti-proliferative and apoptotic agents in cancer cells. Hence, the bioactive compounds present in the CLEO might be accountable for these activities (Narayanankutty *et al.*, 2022).

Aim and Objectives

- To identify the phytoconstituents of *Citrus limetta species* in the database.
- To assess the inhibitory potential of the selected phytoconstituents against Arginine Methyl Transferase *in silico*.

METHODOLOGY

Protein arginine methyltransferases (PRMTs) are emerging as attractive therapeutic targets. PRMTs regulate transcription, splicing, RNA biology, the DNA damage response and cell metabolism; these fundamental processes are altered in many diseases. Arginine methylation is a universal post-translational modification (PTM) conserved in all eukaryotic organisms, from yeasts to humans. Among the PRMT members, PRMT1 and PRMT5 play the most prominent contributions to the arginine methylation levels in mammalian cells. In this study PRMT5 protein was focused.

3.1 Retrieval of protein and ligands:

The X-ray crystal structure of human PRMT5 in complex with a substrate and a co-factor (PDB codes: 5FA5 and 6UXX), were retrieved from the RCSB Protein Data Bank (www.rcsb.org). The ligands (*Citrus limetta* phytochemicals) used for the study (Table 1) were retrieved from PubChem database.

S.No.	<i>Citrus limetta</i> phytochemicals	Molecular formula	Molecular weight (g/mol)
1	Tangeretin	<u>C₂₀H₂₀O₇</u>	372.4
2	Sinensetin	<u>C₂₀H₂₀O₇</u>	372.4
3	Quercetin	<u>C₁₅H₁₀O₇</u>	302.23
4	Nobiletin	<u>C₂₁H₂₂O₈</u>	402.4
5	Myricetin	<u>C₁₅H₁₀O₈</u>	318.23
6	Limocitrol	<u>C₁₈H₁₆O₉</u>	376.3
7	Kaempferol	<u>C₁₅H₁₀O₆</u>	286.24
8	Eriocitrin	<u>C₂₇H₃₂O₁₅</u>	596.5
9	Apigenin_7_glucoside	<u>C₂₁H₂₀O₁₀</u>	432.4
10	Phytoene	<u>C₄₀H₆₄</u>	544.9
11	Luteolin	<u>C₁₅H₁₀O₆</u>	286.24
12	Hesperidin	<u>C₂₈H₃₄O₁₅</u>	610.6
13	Chrysoeriol_6,8_di_c_glucoside	<u>C₂₈H₃₂O₁₆</u>	624.5

Table 1: Molecular formula and molecular weight of selected ligands

3.2 Molecular docking:

Molecular docking was performed mainly by using AutoDock 4.2.6. The proteins 5FA5 and 6UXX were docked with the compounds mentioned in the table 1. All input files were prepared using the AutoDockTools (ADT) 1.5.4 package. To carry out the docking simulations,

a 40 Å × 40 Å × 40 Å grid box with a lattice spacing of 0.375 Å. The grid box enclosed fully the catalytic center of PRMT5. The AutoGrid program was used to construct the grid maps for energy minimization and scoring.

3.3 Docking analysis using AutoDock 4.2.6:

These clusters were ranked by relative binding energy. The poses of the lowest energy (optimal configurations) or the cluster of the largest sizes (suboptimal conformation) were chosen for further analyses in the AutoDock 4.2.6.

3.4 Drug likeliness, ADMET property and Bioactivity score:

Drug likeliness and ADMET properties of the selected ligands were studied using Swiss ADME and admetSAR. Toxicity prediction was performed using Protox II software. Bioactivity score was obtained from Molinspiration software version 2011.06.

3.5 Docking interaction analysis:

The docking interactions were visualized using Biovia Discovery Studio Visualizer software.

RESULTS AND DISCUSSION

In silico approaches have proved to involve less time and cost-effective techniques in drug design and discovery. In the development of new drug candidates against PRMT5 target, several *in silico* studies like structure-based, ligand-based virtual screening, and molecular docking studies were proposed earlier which resulted in various lead inhibitors showing effective binding affinity by means of docking scores, binding free energies, and improved biological activities to PRMT5 target protein.

4.1 Molecular docking:

The crystal structures of proteins 5FA5 and 6UXX were retrieved from Protein Data Bank (PDB) (Figure 1).

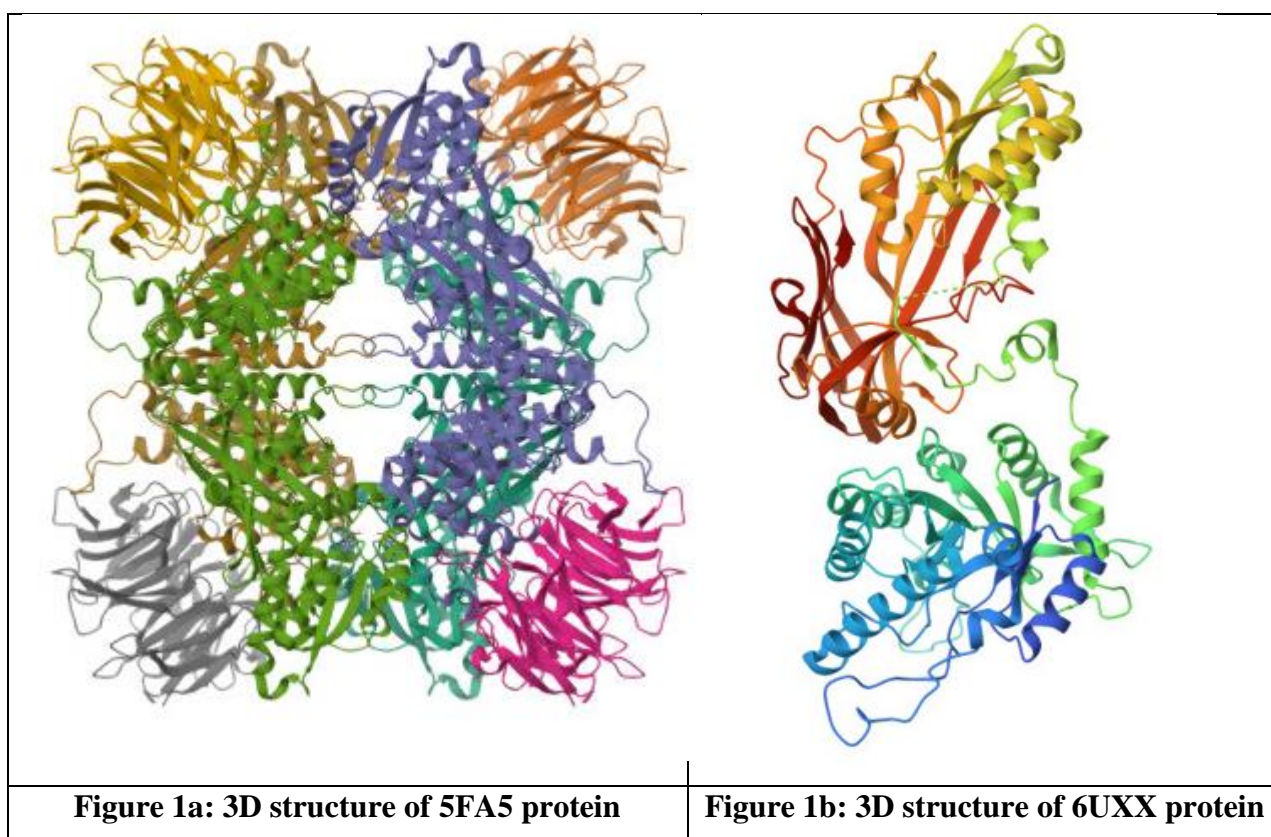


Figure 1: 3D structures of PRMT5 proteins

The 2d structures of *Citrus limetta* compounds were downloaded from PubChem databases. A total of 39 compounds from the plant *Citrus limetta* were docked against two PRMT5 proteins such as 5FA5 and 6UXX. Out of that about 13 compounds were found to show highest negative binding energies in the range of -4.71 to -9.11 (Apigenin 7 glucoside) for 5FA5 and -6.48 to -11.09 (Phytoene) for 6UXX proteins respectively.

Table 2: Drug likeliness and physicochemical properties of the ligands chosen for docking

S.NO	COMPOUNDS	BINDING ENERGY	
		5FA5	6UXX
1.	Tangeretin	-8.05	-7.87
2.	Sinensetin	-8.94	-7.6
3.	Quercetin	-8.27	-8.57
4.	Nobiletin	-8.37	-7.86
5.	Myricetin	-7.92	-7.68
6.	Limocitrol	-7.15	-7.33
7.	Kaempferol	-7.96	-8.41
8.	Eriocitrin	-8.33	-6.88
9.	Apigenin_7_glucoside	-9.11	-9.54
10.	Phytoene	-5.81	-11.09
11.	Luteolin	-5.97	-8.88
12.	Hesperidin	-4.71	-8.37
13.	Chrysoeriol 6,8 di c glucoside	-7.46	-6.48

Molecular docking identifies the best fit between protein and ligands for their structure. The compounds docked with 5FA5 showing highest negative binding energy were apigenin 7 glucoside, sinensetin, nobiletin, quercetin, tangeretin and eriocitrin. The best compounds docked with 6UXX were phytoene, apigenin 7 glucoside, luteolin, hesperidin, kaempferol, quercetin, nobiletin and tangeritin. The binding energy values of these compounds were given in Table 2. Among those compounds apigenin 7 glucoside and phytoene docked with 5FA5 and 6UXX have a highest negative binding energy of -9.11 and -11.09 respectively.

4.2 Drug likeliness and Physicochemical properties of ligands:

The 13 best compounds with highest negative binding energies are Tangeretin, Sinensetin, Quercetin, Nobiletin, Myricetin, Limocitrol, Kaempferol, Eriocitrin, Apigenin_7_glucoside, Phytoene, Luteolin, Hesperidin and Chrysoeriol_6,8_di_c_glucoside. These compounds were analysed for drug likeliness and physiochemical properties.

Table 3: Drug likeliness and physicochemical properties of the ligands chosen for docking

S.No	Compounds	MW g/mol	HA	RB	HBA	HBD	MR	TPSA Å ²	XLOGP ₃	WLOGP	MLOGP	Lipinski violation	Ghose violation	Veber violation	Egan violation	Muegge violation
1.	Tangeretin	372.37	27	6	7	0	100.38	76.36 Å ²	3.04	3.50	0.63	0	0	0	0	0
2.	Sinensetin	372.37	27	6	7	0	100.38	76.36 Å ²	3.50	3.50	0.63	0	0	0	0	0
3.	Quercetin	302.24	22	1	7	5	78.03	131.36 Å ²	1.54	1.99	-0.56	0	0	0	0	0
4.	Nobiletin	402.39	29	7	8	0	106.87	85.59 Å ²	3.01	3.51	0.34	0	0	0	0	0
5.	Myricetin	318.24	23	1	8	6	80.06	151.59 Å ²	1.18	1.69	-1.08	1	0	1	1	2
6.	Limocitrol	376.31	27	4	9	4	95.49	138.82 Å ²	2.43	2.31	-0.86	0	0	0	1	0
7.	Kaempferol	286.24	21	1	6	4	76.01	111.13 Å ²	1.90	2.28	-0.03	0	0	0	0	0
8.	Eriocitrin	596.53	42	6	15	9	136.94	245.29 Å ²	-1.35	-1.78	-3.24	3	4	1	1	3
9.	Apigenin_7_gluco side	432.38	31	4	10	6	106.11	170.05 Å ²	1.22	0.05	-1.61	1	0	1	1	2
10.	Phytoene	544.94	40	20	0	0	190.13	0.00 Å ²	0	13.83	0	0	0	0	0	0
11.	Luteolin	286.24	21	1	6	4	76.01	111.13 Å ²	2.53	2.28	-0.03	0	0	0	0	0
12.	Hesperidin	610.56	43	7	15	8	141.41	234.29 Å ²	-0.14	-1.48	-3.04	3	4	1	1	4
13.	Chrysoeri ol_6,8_di c_gluco side	624.54	44	6	16	11	145.72	280.43 Å ²	-2.28	-3.03	-4.77	3	4	1	1	5

A good drug candidate must obey Lipinski rule of 5, Ghose, Veber, Egan and Moegge rules. Many compounds obeyed Lipinski rule, except eriocitrin, hesperidin and chrysoeriol 6,8 di c glucoside. All the compounds obeyed the other rules, so that the selected ligands were found to possess good drugability properties.

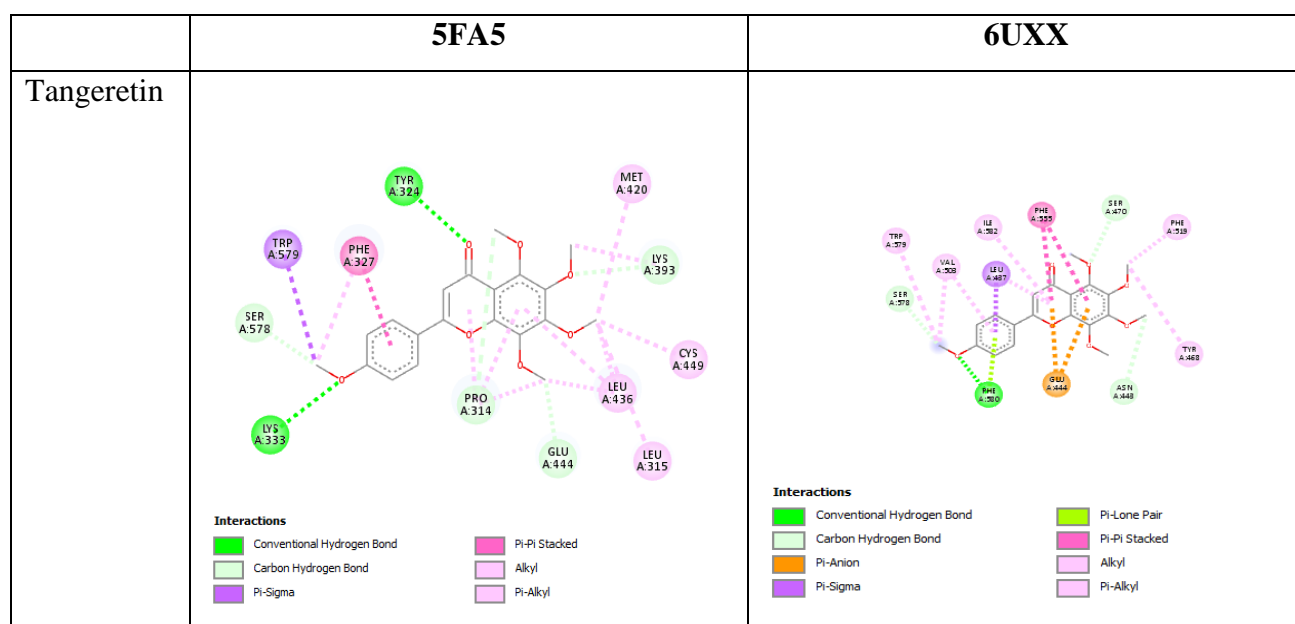
Pharmacokinetic properties are essential in determining the absorption, distribution, metabolism, and excretion of drug molecules. This prediction was done using admetSAR (<http://lmmd.ecust.edu.cn/admetSar1/>; <http://lmmd.ecust.edu.cn/admetSar2/>) versions 1 and 2 and SwissADME (<http://www.swissadme.ch/>) (Cao *et al.*, 2012; Daina *et al.*, 2014; 2017; Daina & Zoete, 2016). Lipinski's oral drug likeliness properties were predicted using the PubChem database. This includes i) Molecular weight (<500 Daltons), ii) Number of hydrogen bond donors (<5), iii) Number of hydrogen bond acceptors (<10), iv) Log P (<5), and v) Molar refractivity (<140) (Lipinski, 2000; 2004). The toxicity properties of ligands were assessed through the EPA's Toxicity Estimation Software Tool 4.2.1 software (Benfenati *et al.*, 2009).

The pharmacokinetic properties were predicted for the top 10 ligands that showed the best binding energy and the drugs that are currently investigated for a potential cure against SARS-CoV-2.

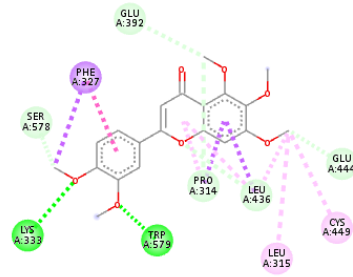
Lipinski rule is considered one of the essential criteria to predict the oral drug likeliness of a drug. Pharmacokinetic and Lipinski properties of the top 10 best potential antiviral ligands were predicted, studied, and tabulated. It is clear that except (-)-solenolide A and rhinacanthin E, none penetrated the Blood-brain barrier. Mitochondria is the subcellular location for the distribution of all the compounds after entering the human body. (-)-Solenolide A, ginkgetin, rhinacanthin E, sorbarin, and betulinic acid satisfied their properties according to Lipinski's rule of 5 (Benet *et al.*, 2016).

4.3 Docking interaction analysis:

The docking interactions of selected ligands with proteins (5FA5 and 6UXX) were given in the table 4. The 2D interaction diagram reveals that all the compounds showed strong polar bonding with the protein which shows the stability of the protein ligand complex.

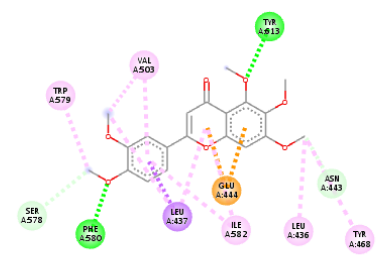


Sinenetin



Interactions

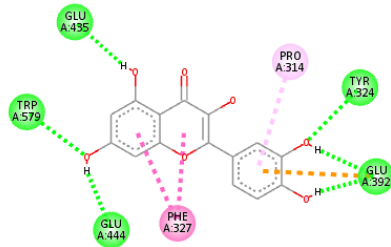
- | | |
|----------------------------|------------------|
| Conventional Hydrogen Bond | Amide-Pi Stacked |
| Carbon Hydrogen Bond | Alkyl |
| Pi-Sigma | Pi-Alkyl |
| Pi-Pi Stacked | |



Interactions

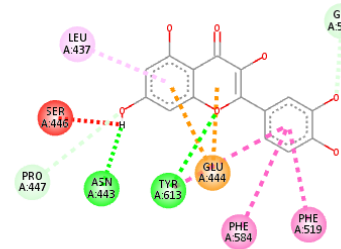
- | | |
|----------------------------|----------|
| Conventional Hydrogen Bond | Pi-Sigma |
| Carbon Hydrogen Bond | Alkyl |
| Pi-Anion | Pi-Alkyl |

Quercetin



Interactions

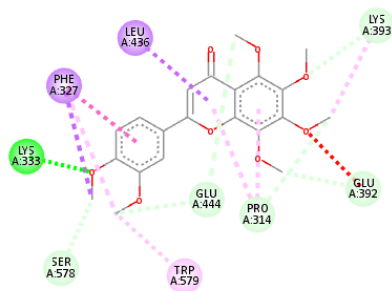
- | | |
|----------------------------|---------------|
| Conventional Hydrogen Bond | Pi-Pi Stacked |
| Carbon Hydrogen Bond | Pi-Alkyl |
| Pi-Anion | |



Interactions

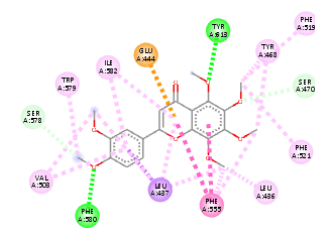
- | | |
|----------------------------|----------------|
| Conventional Hydrogen Bond | Pi-Pi Stacked |
| Carbon Hydrogen Bond | Pi-Pi T-shaped |
| Unfavorable Donor-Donor | Pi-Alkyl |
| Pi-Anion | |

Nobiletin



Interactions

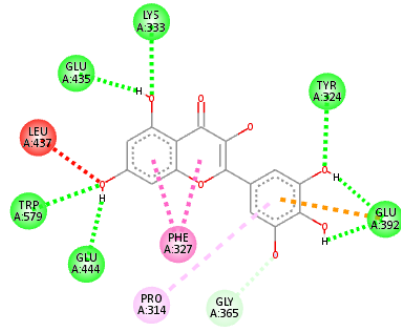
- | | |
|-------------------------------|---------------|
| Conventional Hydrogen Bond | Pi-Pi Stacked |
| Carbon Hydrogen Bond | Alkyl |
| Unfavorable Acceptor-Acceptor | Pi-Alkyl |
| Pi-Sigma | |



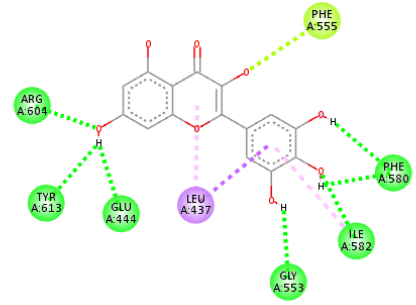
Interactions

- | | |
|----------------------------|---------------|
| Conventional Hydrogen Bond | Pi-Pi Stacked |
| Carbon Hydrogen Bond | Alkyl |
| Pi-Anion | Pi-Alkyl |
| Pi-Sigma | |

Myricetin

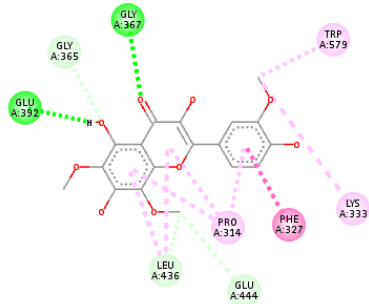


- Interactions**
- Conventional Hydrogen Bond
 - Carbon Hydrogen Bond
 - Unfavorable Acceptor-Acceptor
 - Pi-Anion
 - Pi-Pi Stacked
 - Pi-Alkyl

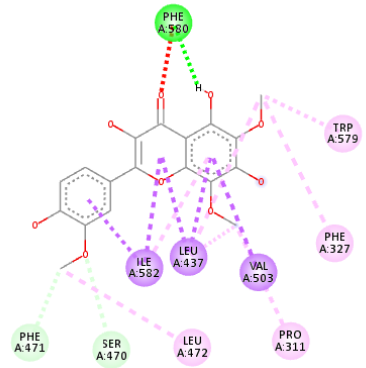


- Interactions**
- Conventional Hydrogen Bond
 - Pi-Sigma
 - Pi-Lone Pair
 - Pi-Alkyl

Limocitrol



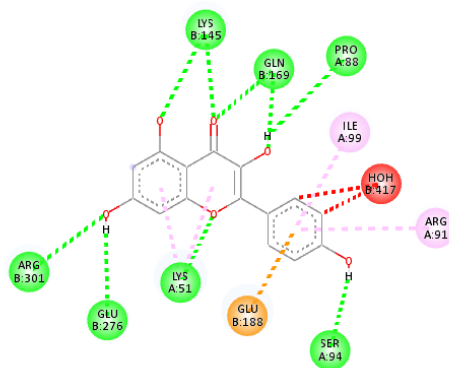
- Interactions**
- Conventional Hydrogen Bond
 - Carbon Hydrogen Bond
 - Pi-Pi Stacked
 - Alkyl
 - Pi-Alkyl



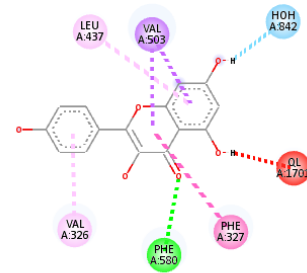
- Interactions**
- Conventional Hydrogen Bond
 - Carbon Hydrogen Bond
 - Unfavorable Acceptor-Acceptor
 - Pi-Sigma
 - Alkyl
 - Pi-Alkyl

Kaempfero

1

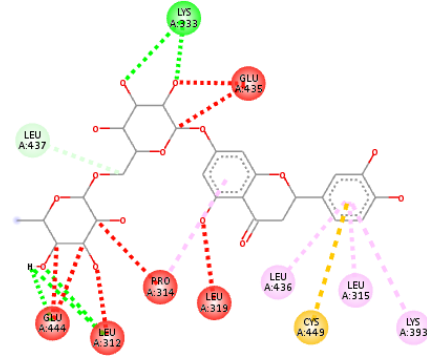


- Interactions**
- Unfavorable Bump
 - Conventional Hydrogen Bond
 - Pi-Anion
 - Pi-Alkyl

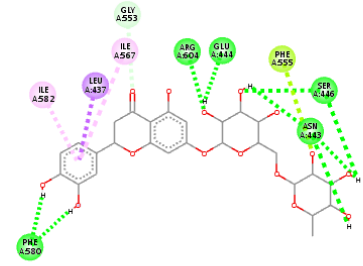


- Interactions**
- Water Hydrogen Bond
 - Conventional Hydrogen Bond
 - Unfavorable Donor-Donor
 - Pi-Sigma
 - Pi-Pi T-shaped
 - Pi-Alkyl

Eriocitrin

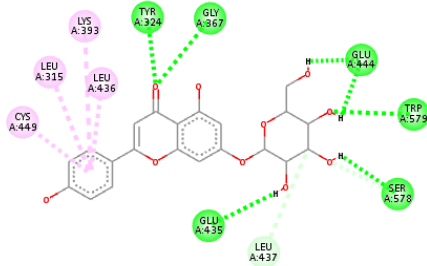


- Interactions**
- Unfavorable Bump
 - Conventional Hydrogen Bond
 - Carbon Hydrogen Bond
 - Pi-Sulfur
 - Pi-Alkyl

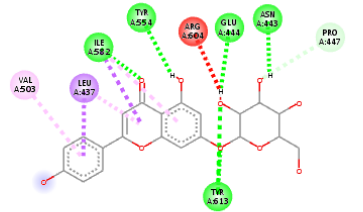


- Interactions**
- Conventional Hydrogen Bond
 - Carbon Hydrogen Bond
 - Pi-Sigma
 - Pi-Lone Pair
 - Pi-Alkyl

Apigenin_7_glucosid e

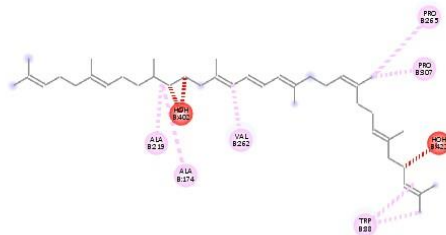


- Interactions**
- Conventional Hydrogen Bond
 - Carbon Hydrogen Bond
 - Pi-Alkyl

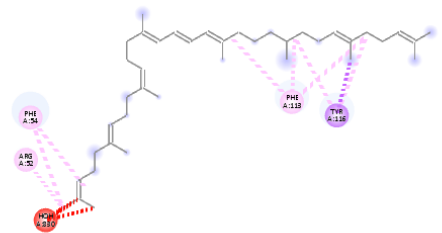


- Interactions**
- Conventional Hydrogen Bond
 - Carbon Hydrogen Bond
 - Unfavorable Donor-Donor
 - Pi-Sigma
 - Pi-Alkyl

Phytoene



- Interactions**
- Unfavorable Bump
 - Pi-Sigma
 - Alkyl
 - Pi-Alkyl



- Interactions**
- Unfavorable Bump
 - Pi-Sigma
 - Alkyl
 - Pi-Alkyl

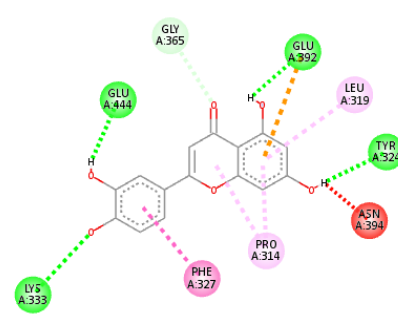
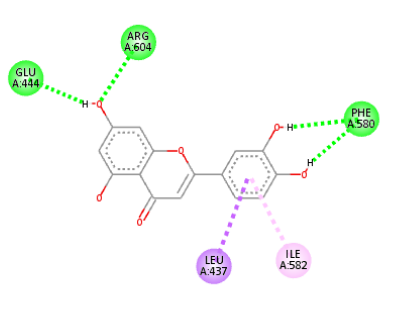
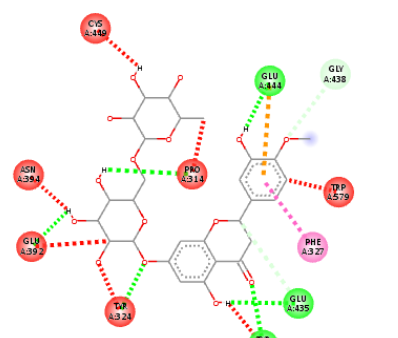
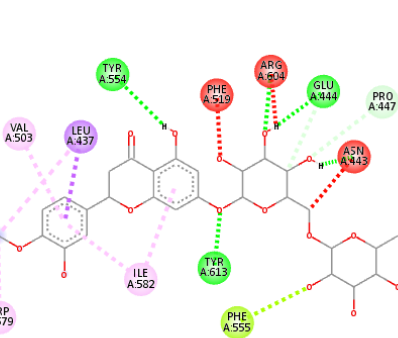
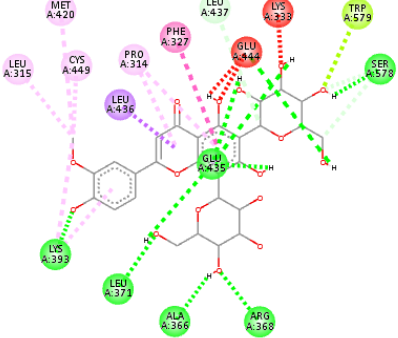
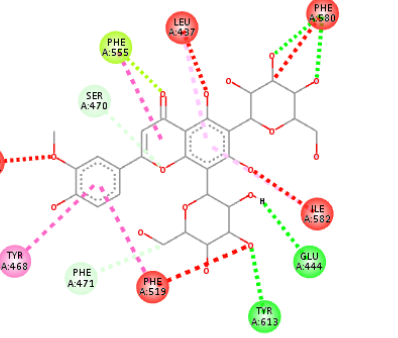
<p>Luteolin</p>	 <p>Interactions</p> <ul style="list-style-type: none"> Conventional Hydrogen Bond Carbon Hydrogen Bond Unfavorable Donor-Donor Pi-Anion Pi-Pi Stacked Pi-Alkyl 	 <p>Interactions</p> <ul style="list-style-type: none"> Conventional Hydrogen Bond Pi-Sigma Pi-Alkyl
<p>Hesperidin</p>	 <p>Interactions</p> <ul style="list-style-type: none"> Unfavorable Bump Conventional Hydrogen Bond Carbon Hydrogen Bond Unfavorable Donor-Donor Pi-Anion Pi-Pi T-shaped 	 <p>Interactions</p> <ul style="list-style-type: none"> Unfavorable Bump Conventional Hydrogen Bond Carbon Hydrogen Bond Pi-Sigma Pi-Lone Pair Alkyl Pi-Alkyl
<p>Chrysoerio l_6,8_di_c _glucoside</p>	 <p>Interactions</p> <ul style="list-style-type: none"> Unfavorable Bump Conventional Hydrogen Bond Carbon Hydrogen Bond Pi-Sigma Pi-Lone Pair Pi-Pi Stacked Alkyl Pi-Alkyl 	 <p>Interactions</p> <ul style="list-style-type: none"> Unfavorable Bump Conventional Hydrogen Bond Carbon Hydrogen Bond Pi-Lone Pair Pi-Pi Stacked Pi-Pi T-shaped Pi-Alkyl

Table 4: Docking interaction analysis of the selected ligands with 5FA5 and 6UXX:

All compounds formed pi-pi interactions with Phe327 aminoacid in the 5FA5 protein except eriocitrin and apigenin 7 glucoside. Similarly, in 6UXX all compounds formed pi-pi interactions with Phe327 aminoacid except sinensetin. All the compounds formed conventional hydrogen bond and carbon hydrogen bond with various aminoacids (TYR-324, LYS-333, TRP-579, GLU-435, GLU-444, GLU-392, GLY-392, GLY-367, SER-578, TYR-334, LYS-393, LEU-371, ALA-366, ARG-368, SER-578, PRO-314, LEU-436, GLY-365, GLY-438, LEU-437, SER-470, ASN-443, PRO-447, GLY-553, PHE-580, TYR-613, ARG-604, ILE-582, PHE-471) such as in both the proteins. Compounds like tangeretin, sinensetin, nobiletin, chrysoeriol_6,8-di_c_glucoside formed Pi-sigma bond with (TRP-579, PHE-327, LEU-436) present in 5FA5 protein. Compounds like tangeretin, sinensetin, nobiletin, myricetin, limocitrol, eriocitrin, luteolin, hesperidin formed Pi-sigma bond with (LEU-380, LEU-437, ILE-582, VAL-503) present in 6UXX protein.

Table 5 shows the results of ADMET properties of the selected compounds. ADMET analysis was performed to check the absorption, distribution, metabolism, excretion and toxicity of the selected ligands. ADMET properties can be predicted using various softwares such as SwissADME and admetSAR. The results reveal that human intestinal absorption of the compounds such as tangeretin, sinensetin, quercetin, nobiletin, myricetin, limocitrol, kaempferol, apigenin 7 glucoside, phytoene and luteolin were better (more than 90%). The plasma protein binding of a good drug candidate must be less than 90%. The compounds obeying these category are apigenin 7 glucoside, phytoene, luteolin and hesperidin. No compounds inhibited CYP2D6 enzyme which is an important enzyme involved in drug metabolism.

Toxicity analysis of compounds can be predicted using ProTox-II software ProTox-II, which is a freely available computational toxicity webserver enabling the prediction of the largest number of toxicity endpoints. Toxicity analysis results reveal that no compounds showed carcinogenicity and mutagenicity. All the top lead molecules showed negative test for mutagenic and carcinogenic in Protox II prediction including the final potential leads to phytoene and Apigenin_7_glucoside. All the identified lead molecules were showing similar toxicity profile considering their more drug-like properties.

Table 5: ADMET properties of the selected ligands

Compounds	Absorption	Distribution	Metabolism	Excretion	Toxicity	
	HIA	PPB	CYP2D6 inhibitor	Total clearance	Mutagenicity	Carcinogenicity
Tangeretin	99%	90%	No	3.949	NM	NC
Sinensetin	99%	93%	No	5.809	NM	NC
Quercetin	91%	17%	No	8.284	NM	NC
Nobiletin	99%	92%	No	4.605	NM	NC
Myricetin	91%	99%	No	0	NM	NC
Limocitrol	94%	91%	No	2.529	NM	NC
Kaempferol	95%	20%	No	6.868	NM	NC
Eriocitrin	56%	90%	No	0	NM	NC
Apigenin_7_glucoside	95%	89%	No	2.878	NM	NC
Phytoene	99%	68%	No	2.908	NM	NC
Luteolin	91%	11%	No	8.146	NM	NC
Hesperidin	48%	85%	No	0	NM	NC
Chrysoeriol_6,8_di_c_glucoside	61%	64%	No	0	NM	NC

The bioactivity scores prediction of the selected compounds against the 5FA5 and 6UXX proteins based on the calculation of the GPCR ligand, ion channel modulation, kinase inhibitor, nuclear receptor ligand, protease inhibition and enzyme inhibition towards drug likeliness is scored and presented in Table 6.

The bioactivity scores were calculated using a signaling cascade that included GPCR ligands, ion channel modulators, protein kinase inhibitors, nuclear receptor ligands, and protease inhibitor ligands. GPCR ligand-based signaling cascade was used to develop a new functional drug with an increased binding selectivity profile and less undesirable effects. Ion channel modulators allow the movement of charged particles across cell membranes and are essential therapeutic targets modulated by various medicinal drugs. For developing selective inhibitors to block or modulate diseased signaling pathways, Kinase inhibitors are considered a promising approach for drug development.

Table 6: Bioactivity scores of selected ligands

S. No	Compounds	GPCR Receptor	Ion channel modulator	Protein Kinase Inhibitor	Nuclear Receptor	Protease Inhibitor	Enzyme inhibitor
1	Tangeretin	-0.12	-0.04	-0.14	0.03	-0.20	0.11
2	Sinensetin	-0.08	-0.15	-0.06	0.10	-0.20	0.10
3	Quercetin	-0.06	-0.19	0.03	0.36	-0.25	0.28
4	Nobiletin	-0.13	-0.04	-0.13	0.00	-0.22	0.11
5	Myricetin	-0.06	-0.18	0.08	0.32	-0.20	0.30
6	Limocitrol	-0.20	-0.21	-0.2	-0.03	-0.36	0.19
7	Kaempferol	-0.10	-0.21	-0.06	0.32	-0.27	0.26
8	Eriocitrin	0.06	-0.47	-27.95	-0.08	0.05	0.16
9	Apigenin_7_glu coside	0.10	-0.01	0.16	0.31	0.02	0.43
10	Phytoene	0.06	-0.16	-0.11	0.16	-0.01	0.09
11	Luteolin	-0.02	-0.07	0.04	0.39	-0.22	0.28
12	Hesperidin	-0.01	-0.59	-0.36	-0.20	-0.00	0.06
13	Chrysoeriol_6,8 _di_c_glucoside	-0.08	-0.66	-0.29	-0.26	-0.07	0.03

The bioactive scores fall on the following ranges such as active > 0, moderately active -5.0 to 0.0 and inactive < -5.0. The bioactivity analysis revealed that all the compounds were moderately bioactive in which Luteolin and apigenin 7 glucoside showed better results.

In conclusion luteolin found to interact better with 5FA5 and 6UXX. Though sinensetin could interact with the proteins with better binding energy, it violated the Lipinski rule of 5, PPB was also more 90% and the bioactivity score was also very less considering it a less drug-like compound. Thus, based on the physio-chemical properties, Luteolin scores to be the best candidate in targeting PRMT5 protein, among the phytoconstituents of the Citrus fruit chosen from the databases.

SUMMARY AND CONCLUSION

In silico approaches have proved to involve less time and cost-effective techniques in drug design and discovery. In the development of new drug candidates against PRMT5 target, several *in silico* studies like structure-based, ligand-based virtual screening, and molecular docking studies were proposed earlier which resulted in various lead inhibitors showing effective binding affinity by means of docking scores, binding free energies, and improved biological activities to PRMT5 target protein.

The crystal structures of proteins were retrieved from Protein Data Bank (PDB). The 2d structures of *Citrus limetta* compounds were downloaded from PubChem databases. A total of 39 compounds from the plant *Citrus limetta* were docked against two PRMT5 proteins such as 5FA5 and 6UXX. Out of that about 13 compound were found to show highest negative binding energies in the range of -4.71 to -9.11 (Apigenin 7 glucoside) for 5FA5 and -6.48 to -11.09 (Phytoene) for 6UXX proteins respectively.

Molecular docking identifies the best fit between protein and ligands for their structure. The best compounds docked with 5FA5 and 6UXX were apigenin 7 glucoside and phytoene with a highest negative binding energy of -9.11 and -11.09 respectively followed by Luteolin.

The 13 best compounds with highest negative binding energies are Tangeretin, Sinensetin, Quercetin, Nobiletin, Myricetin, Limocitrol, Kaempferol, Eriocitrin, Apigenin_7_glucoside, Phytoene, Luteolin, Hesperidin and Chrysoeriol_6,8_di_c_glucoside. These compounds were analysed for drug likeliness and physiochemical properties.

A good drug candidate must obey Lipinski rule of 5, Ghose, Veber, Egan and Moegge rules. Many compounds obeyed Lipinski rule, except eriocitrin, hesperidin and chrysoeriol 6,8 di c glucoside. All the other compounds analysed obeyed the other rules, so that the selected ligands were found to possess good drugability properties.

The docking interactions of selected ligands with proteins (5FA5 and 6UXX) were given in the table 4. The 2D interaction diagram reveals that all the compound showed strong polar bonding with the protein which shows the stability of the protein ligand complex.

ADMET analysis was performed to check the absorption, distribution, metabolism, excretion and toxicity of the selected ligands. ADMET properties can be predicted using various softwares such as SwissADME and admetSAR. The results reveal that human intestinal absorption of the compounds such as tangeretin, sinensetin, quercetin, nobiletin, myricetin, limocitrol, kaempferol, apigenin 7 glucoside, phytoene, hesperidin and luteolin were better (more than 90%). The plasma protein binding of a good drug candidate must be less than 90%. The compounds obeying these category are apigenin 7 glucoside, phytoene and hesperidin. No

compounds inhibited CYP2D6 enzyme which is an important enzyme involved in drug metabolism. Toxicity analysis of compounds can be predicted using ProTox-II software ProTox-II, which is a freely available computational toxicity webserver enabling the prediction of the largest number of toxicity endpoints. Toxicity analysis results reveal that no compounds showed carcinogenicity and mutagenicity. All the top lead molecules showed negative test for mutagenic and carcinogenic in Protox II prediction including the final potential leads to phytoene and Apigenin_7_glucoside. All the identified lead molecules were showing similar toxicity profile considering their more drug-like properties. The bioactivity analysis revealed that all the compounds were moderately bioactive in which apigenin 7 glucoside and luteolin showed better results.

Thus it can be concluded that, Luteolin exhibit more drug-likeness for the treatment and therapy for leukemia based on PRMT5(Arginine Methyl Transferase) inhibition strategy. Further biochemical analysis has to be performed to analyse the drug efficacy of the molecule against leukemia.

BIBLIOGRAPHY

Antonyamy S, Bonday Z, Campbell RM, Doyle B, Druzina Z, Gheyi T, Han B, Jungheim LN, Qian Y, Rauch C, Russell M, Sauder JM, Wasserman SR, Weichert K, Willard FS, Zhang A, Emtage S (2012) Crystal structure of the human PRMT5:MEP50 complex. *Proc Natl Acad Sci U S A* 109:17960–17965

Awan, F.T., Al-Sawaf, O., Fischer, K. and Woyach, J.A., 2020. Current perspectives on therapy for chronic lymphocytic leukemia. *American Society of Clinical Oncology Educational Book*, 40, pp.320-329

Banerjee, P., Eckert, A.O., Schrey, A.K. and Preissner, R., 2018. ProTox-II: a webserver for the prediction of toxicity of chemicals. *Nucleic acids research*, 46(W1), pp.W257-W263.

Bhowal, R., Kumari, S., Sarma, C., Suprasanna, P. and Roy, P., 2022. Phytochemical Constituents and Bioactivity Profiles of Citrus Genus from India. *Analytical Chemistry Letters*, 12(6), pp.770-787.

Burgos, E.S., Wilczek, C., Onikubo, T., Bonanno, J.B., Jansong, J., Reimer, U. and Shechter, D., 2015. Histone H2A and H4 N-terminal tails are positioned by the MEP50 WD repeat protein for efficient methylation by the PRMT5 arginine methyltransferase. *Journal of Biological Chemistry*, 290(15), pp.9674-9689.

Chan-Penebre, E., Kuplast, K.G., Majer, C.R., Boriack-Sjodin, P.A., Wigle, T.J., Johnston, L.D., Rioux, N., Munchhof, M.J., Jin, L., Jacques, S.L. and West, K.A., 2015. A selective inhibitor of PRMT5 with in vivo and in vitro potency in MCL models. *Nature chemical biology*, 11(6), pp.432-437.

Chen, Y., Shao, X., Zhao, X., Ji, Y., Liu, X., Li, P., Zhang, M. and Wang, Q., 2021. Targeting protein arginine methyltransferase 5 in cancers: Roles, inhibitors and mechanisms. *Biomedicine & Pharmacotherapy*, 144, p.112252.

Fan, J., Fu, A. and Zhang, L., 2019. Progress in molecular docking. *Quantitative Biology*, 7, pp.83-89.

Frank, R.C., 2013. *Fighting Cancer with Knowledge and Hope: A Guide for Patients, Families, and Health Care Providers*. Yale University Press

Fu, S., Zheng, Q., Zhang, D., Lin, C., Ouyang, L., Zhang, J. and Chen, L., 2022. Medicinal chemistry strategies targeting PRMT5 for cancer therapy. *European Journal of Medicinal Chemistry*, p.114842.

Fulton, M.D., Dang, T., Brown, T. and Zheng, Y.G., 2022. Effects of substrate modifications on the arginine dimethylation activities of PRMT1 and PRMT5. *Epigenetics*, 17(1), pp.1-18.

Gu, Z., Gao, S., Zhang, F., Wang, Z., Ma, W., Davis, R.E. and Wang, Z., 2012. Protein arginine methyltransferase 5 is essential for growth of lung cancer cells. *Biochemical Journal*, 446(2), pp.235-241.

Hehlmann, R., 2020. Chronic myeloid leukemia in 2020. *Hemasphere*, 4(5).

Karkhanis, V., Hu, Y.J., Baiocchi, R.A., Imbalzano, A.N. and Sif, S., 2011. Versatility of PRMT5-induced methylation in growth control and development. *Trends in biochemical sciences*, 36(12), pp.633-641

Kato, M. and Manabe, A., 2018. Treatment and biology of pediatric acute lymphoblastic leukemia. *Pediatrics International*, 60(1), pp.4-12

Lin, H. and Luengo, J.I., 2019. Nucleoside protein arginine methyltransferase 5 (PRMT5) inhibitors. *Bioorganic & Medicinal Chemistry Letters*, 29(11), pp.1264-1269.

Lin, H., Wang, M., Zhang, Y.W., Tong, S., Leal, R.A., Shetty, R., Vaddi, K. and Luengo, J.I., 2019. Discovery of and selective covalent protein arginine methyltransferase 5 (PRMT5) inhibitors. *ACS Medicinal Chemispotent try Letters*, 10(7), pp.1033-1038.

Lohidakshan, K., Rajan, M., Ganesh, A., Paul, M. and Jerin, J., 2018. Pass and Swiss ADME collaborated in silico docking approach to the synthesis of certain pyrazoline spacer compounds for dihydrofolate reductase inhibition and antimalarial activity. */// Bangladesh Journal of Pharmacology///*, 13(1), pp.23-29.

López Simeon, R., *Capacidad antibacteriana de Oedogonium capillare, Citrus limon y Mangifera indica como control de infecciones bacterianas en Carassius auratus* (Doctoral dissertation, Universidad Autónoma Metropolitana. Unidad Xochimilco).

Luque Cutipa, V.R. and Mendiguete García, M.C., 2021. Actividad antibacteriana in vitro del extracto etanólico de la cáscara de *Citrus limetta* risso (lima) frente a *Staphylococcus aureus* ATCC 25923.

Mattiuzzi, C. and Lippi, G., 2019. Current cancer epidemiology. *Journal of epidemiology and global health*, 9(4), p.217.

Mavrakis, K.J., McDonald III, E.R., Schlabach, M.R., Billy, E., Hoffman, G.R., deWeck, A., Ruddy, D.A., Venkatesan, K., Yu, J., McAllister, G. and Stump, M., 2016. Disordered methionine metabolism in MTAP/CDKN2A-deleted cancers leads to dependence on PRMT5. *Science*, 351(6278), pp.1208-1213

Meijers, W.C. and de Boer, R.A., 2019. Common risk factors for heart failure and cancer. *Cardiovascular research*, 115(5), pp.844-853. Mattiuzzi, C., & Lippi, G. (2019). Current cancer epidemiology. *Journal of epidemiology and global health*, 9(4), 217.

Miller, K.D., Nogueira, L., Mariotto, A.B., Rowland, J.H., Yabroff, K.R., Alfano, C.M., Jemal, A., Kramer, J.L. and Siegel, R.L., 2019. Cancer treatment and survivorship statistics, 2019. *CA: a cancer journal for clinicians*, 69(5), pp.363-385. Lin, H., Wang, M., Zhang, Y. W., Tong, S., Leal, R. A., Shetty, R., ... & Luengo, J. I. (2019). Discovery of potent and selective covalent protein arginine methyltransferase 5 (PRMT5) inhibitors. *ACS Medicinal Chemistry Letters*, 10(7), 1033-1038.

Mishra, S. and Dahima, R., 2019. In vitro ADME studies of TUG-891, a GPR-120 inhibitor using SWISS ADME predictor. *Journal of drug delivery and therapeutics*, 9(2-s), pp.366-369.

Moon, A.R.C.H.A.N.A., Khan, D.E.E.B.A., Gajbhiye, P.R.A.N.J.A.L.I. and Jariya, M., 2017. Insilico prediction of toxicity of ligands utilizing admetsar. *Int. J. Pharma. Bio. Sci*, 8, pp.674-677.

Narayanankutty, A., Visakh, N.U., Sasidharan, A., Pathrose, B., Olatunji, O.J., Al-Ansari, A., Alfarhan, A. and Ramesh, V., 2022. Chemical Composition, Antioxidant, Anti-Bacterial, and Anti-Cancer Activities of Essential Oils Extracted from *Citrus limetta* Risso Peel Waste Remains after Commercial Use. *Molecules*, 27(23), p.8329.

Ndombera, F., Maiyoh, G. and Tuei, V., 2019. Pharmacokinetic, physicochemical and medicinal properties of n-glycoside anti-cancer agent more potent than 2-deoxy-d-glucose in lung cancer cells.

Pal, S., Vishwanath, S.N., Tempst, P., Sif, S. and Erdjument-bromage, H., 2004. Negatively regulates expression of ST7 and NM23 tumor suppressor genes human SWI/SNF-associated PRMT5 methylates histone H3 arginine 8 and negatively regulates expression of ST7 and NM23 tumor suppressor genes. *Mol. Cell. Biol.*, 24(21), pp.9630-9645.

Palte, R.L., Schneider, S.E., Altman, M.D., Hayes, R.P., Kawamura, S., Lacey, B.M., Mansueto, M.S., Reutershan, M., Siliphaivanh, P., Sondey, C. and Xu, H., 2020. Allosteric modulation of protein arginine methyltransferase 5 (PRMT5). *ACS Medicinal Chemistry Letters*, 11(9), pp.1688-1693.

Q. Zhao, G. Rank, Y. T. Tan, H. Li, R. L. Moritz, R. J. Simpson, L. Cerruti, D.J. Curtis, D. J. Patel, C. D. Allis, J. M. Cunningham and S. M. Jane, *Nat.Struct. Mo.l Biol.*, 2009, 16, 304-311.

Rengasamy, M., Zhang, F., Vashisht, A., Song, W.M., Aguilo, F., Sun, Y., Li, S., Zhang, W., Zhang, B., Wohlschlegel, J.A. and Walsh, M.J., 2017. The PRMT5/WDR77 complex regulates alternative splicing through ZNF326 in breast cancer. *Nucleic Acids Research*, 45(19), pp.11106-11120.

Russo, C., Maugeri, A., Lombardo, G.E., Musumeci, L., Barreca, D., Rapisarda, A., Cirmi, S. and Navarra, M., 2021. The second life of Citrus fruit waste: A valuable source of bioactive compounds. *Molecules*, 26(19), p.5991

Sheng, X. and Wang, Z., 2016. Protein arginine methyltransferase 5 regulates multiple signaling pathways to promote lung cancer cell proliferation. *BMC cancer*, 16(1), pp.1-13.

Shilpi, A., Parbin, S., Sengupta, D., Kar, S., Deb, M., Rath, S.K., Pradhan, N., Rakshit, M. and Patra, S.K., 2015. Mechanisms of DNA methyltransferase–inhibitor interactions: Procyanidin B2 shows new promise for therapeutic intervention of cancer. *Chemico-biological interactions*, 233, pp.122-138.

Shivanika, C., Kumar, D., Ragunathan, V., Tiwari, P. and Sumitha, A., 2020. Molecular docking, validation, dynamics simulations, and pharmacokinetic prediction of natural

compounds against the SARS-CoV-2 main-protease. *Journal of biomolecular structure & dynamics*, p.1.

Shyam, J., 2019. The Phytochemical and Pharmacological Activity of Citrus limetta Peel Extracts. *Journal of Global Biosciences*, 8(8), pp.6382-6396.

Stopa, N., Krebs, J.E. and Shechter, D., 2015. The PRMT5 arginine methyltransferase: many roles in development, cancer and beyond. *Cellular and molecular life sciences*, 72, pp.2041-2059.

Sturgeon, K.M., Deng, L., Bluethmann, S.M., Zhou, S., Trifiletti, D.M., Jiang, C., Kelly, S.P. and Zaorsky, N.G., 2019. A population-based study of cardiovascular disease mortality risk in US cancer patients. *European heart journal*, 40(48), pp.3889-3897.

Sulimov, V.B., Kutov, D.C. and Sulimov, A.V., 2019. Advances in docking. *Current medicinal chemistry*, 26(42), pp.7555-7580.

Tyner, J.W., Tognon, C.E., Bottomly, D., Wilmot, B., Kurtz, S.E., Savage, S.L., Long, N., Schultz, A.R., Traer, E., Abel, M. and Agarwal, A., 2018. Functional genomic landscape of acute myeloid leukaemia. *Nature*, 562(7728), pp.526-531

Wang, F., Lv, H., Zhao, B., Zhou, L., Wang, S., Luo, J., Liu, J. and Shang, P., 2019. Iron and leukemia: new insights for future treatments. *Journal of Experimental & Clinical Cancer Research*, 38, pp.1-17.

Wang, F., Lv, H., Zhao, B., Zhou, L., Wang, S., Luo, J., Liu, J. and Shang, P., 2019. Iron and leukemia: new insights for future treatments. *Journal of Experimental & Clinical Cancer Research*, 38, pp.1-17

Yang, Z., Xiao, T., Li, Z., Zhang, J. and Chen, S., 2022. Novel chemicals derived from Tadalafil exhibit PRMT5 inhibition and promising activities against breast cancer. *International Journal of Molecular Sciences*, 23(9), p.4806.

Yang, Z., Xiao, T., Li, Z., Zhang, J. and Chen, S., 2022. Novel chemicals derived from Tadalafil exhibit PRMT5 inhibition and promising activities against breast cancer. *International Journal of Molecular Sciences*, 23(9), p.4806.

Zhu, F. and Rui, L., 2019. PRMT5 in gene regulation and hematologic malignancies. *Genes & Diseases*, 6(3), pp.247-257.

